NUCLEAR GIANT RESONANCES IN A RELATIVISTIC MEAN-FIELD THEORY*

BY R. J. FURNSTAHL AND B. D. SEROT**

Institute of Theoretical Physics, Department of Physics, Stanford University, Stanford, California 94305, USA

(Received November 23, 1984)

Isoscalar and isovector giant resonances in doubly magic nuclei are studied in a relativistic meson-baryon field theory. Time-dependent oscillations about static ground-state configurations are described by linearized equations of motion. Coulomb effects are included. Variational estimates of the solutions to these equations are obtained using relativistic Hartree results to define the equilibrium densities. Energies and transition densities are found for the lowest-lying collective modes, and the systematic dependence of the energies on baryon number is examined.

PACS numbers: 21.60.–n

1. Introduction

To overcome some of the limitations of conventional nuclear structure theory at nuclear and higher densities, a model relativistic quantum field theory has been developed [1]. In this theory, nucleon-nucleon interactions are described by meson exchange rather than static two-body potentials. The constraints of Lorentz covariance, causality, and retardation are incorporated naturally, providing a more complete and satisfactory description of nuclei. Furthermore, the recent success of relativistic calculations of medium-energy nucleon-nucleus scattering [2] gives new evidence that relativistic effects in ordinary nuclei cannot be neglected.

The original model of Walecka [1] consists of a nucleon field ψ, a neutral scalar meson field ϕ coupled to the scalar density $\bar{\psi}\psi$, and a neutral vector meson field V_μ coupled to the conserved baryon current $\bar{\psi}\gamma^\mu\psi$. The model has been extended to include photons, pions, and rho mesons using a renormalizable lagrangian density [3]. This provides a consistent calculational framework in which to do nuclear structure physics. The ground states of doubly magic nuclei have been studied in the self-consistent Hartree approximation to the extended model [4]. Calculated charge densities, neutron densities, rms radii

* Supported in part by NSF grant PHY 81-07395.

** Alfred P. Sloan Foundation Research Fellow. Permanent address: Department of Physics, Indiana University, Bloomington, IN 47405, USA.

and single-particle energy levels throughout the periodic table agree with experiment at the level of the most sophisticated nonrelativistic calculations to date.

Since the relativistic theory successfully describes ground-state and single-particle properties of nuclei, it is of interest to examine its predictions for excited states. Walecka and Horowitz [5, 6] investigated collective excitations in a relativistic mean-field model, using ground-state densities calculated in the Thomas-Fermi approximation. Collective modes were introduced by allowing the mean fields and nucleon densities to acquire a slow time dependence. These modes are expected to describe the main features of nuclear giant resonances. Isoscalar and isovector modes were studied for a model nucleus (baryon number $A = 67.19$) with equal numbers of neutrons N and protons Z, and Coulomb effects were neglected. Reasonable excitation energies and transition densities were obtained for the lowest-lying modes.

In this paper, we extend the procedure of Refs. [5] and [6] to real nuclei and examine the collective modes of excitation. We use self-consistent relativistic Hartree densities [4], which provide a more realistic description of ground-state properties than Thomas-Fermi densities. Nuclei with $N \neq Z$ are considered, in which there is only an approximate separation of the collective motion into isoscalar and isovector components. We also include Coulomb corrections. The model parameters are taken from the ground-state calculations of Ref. [4], and *no new parameters* are introduced to describe the excited states.

In Sects. 2 and 3, we review the formalism developed by Walecka and Horowitz and extend it to include Coulomb effects. One begins by defining a collective variable to describe the local (irrotational) velocity of the nuclear fluid. The nucleon motion modifies the source terms in the meson field equations producing corresponding time-dependent changes in the condensed meson fields. Since the nucleon dynamics is in turn specified by the meson fields, collective modes of nuclear motion arise naturally in this approach. An energy functional is introduced that, when minimized subject to appropriate constraints, reproduces the linearized equations of motion for the meson fields and local hydrodynamic velocities of the nucleons. Previous work [6] shows that variational estimates based on this energy functional are sufficient for studying the properties of the collective modes to an accuracy of 10–20%. The simplicity of the variational approach (as compared with solving the full set of coupled hydrodynamic equations) allows us to examine the systematics of these modes throughout the periodic table. Estimates for the energies of isovector and isoscalar modes in doubly magic nuclei (^{40}Ca, ^{48}Ca, ^{90}Zr, and ^{208}Pb) are summarized in Table II and Figs. 2–4. The systematics of the excitation energies are examined and compared to experimental data on giant resonances in Figs. 5–7. Finally, the transition densities are compared with other (nonrelativistic) calculations in Sect. 5.

We find that the systematics of the giant dipole (1^-) resonance are accurately reproduced in this simple model, and the excitation energies are within 20% of experiment with no adjustment of the parameters determined from ground-state properties. The systematics of the other resonances with respect to nucleon number A are also reasonable, and the energies of the isoscalar quadrupole (2^+) and octupole (3^-) resonances differ from experimental values by approximately 20%.

This paper has three main goals. First, as pointed out in Refs. [5] and [6], the nuclear ground states in this relativistic formalism are described with an interaction that produces Lorentz scalar and four-vector components of approximately several hundred MeV in the nucleon Dirac equation. Delicate cancellations arise between these components in the description of certain static properties, for example, the nuclear binding energy. It is therefore *not* obvious that small deviations in these components will result in reasonable collective-mode energies on the order of tens of MeV. In fact, we find that small oscillations about the static configurations have a reasonable spectrum, and at least with our approximations, no new relativistic effects enter beyond those contained in the ground-state calculations.

Second, the parameters used to describe the ground states are determined primarily from the bulk properties of finite nuclei. The single-particle interaction is extremely simple (it contains only four adjusted parameters), and it leads naturally to a shell-model spectrum for the single-particle levels [4]. Our results show that the same interaction produces reasonable collective-mode spectra, *without any further adjustment of parameters.*

Finally, since the present approach is based on simple, time-dependent mean fields, it is of interest to study the systematic dependence of the mode energies on the baryon number. This is most easily done with a variational calculation. Given the success of our variational results in reproducing these systematics, it is clear that a more detailed study of collective modes in a relativistic framework is needed. This may be done by extending the familiar techniques of the Tamm-Dancoff and random-phase approximations, as we describe briefly in Sect. 6.

2. *Linearized equations of motion*

We describe the nuclear motion by introducing local, irrotational velocity fields $\boldsymbol{v}_p = -\nabla\psi_p(\boldsymbol{x}, t)$ and $\boldsymbol{v}_n = -\nabla\psi_n(\boldsymbol{x}, t)$ for protons and neutrons, respectively. (Departures from irrotational flow are corrections to our approach and have been discussed by Serr, Bertsch, and others [7]). The local hydrodynamic motion of the nucleons changes the sources that determine the classical meson fields. By allowing the fields to develop a time dependence, we may then look for departures from the static field configurations that oscillate with a *well-defined frequency*. Since the nucleon dynamics is in turn determined by the meson fields, collective motion of the nucleons throughout the nucleus arises naturally in response to the oscillating fields. The nucleon motion is locally incoherent (described by the hydrodynamic velocity) but globally coherent due to the time-dependent meson fields. It is therefore reasonable that this picture will provide an approximate description of giant resonances in nuclei.

In nonrelativistic hydrodynamic approaches to giant resonances [8–10], which are known to have limited success, no time dependence is introduced into the nucleon-nucleon interaction. More refined approximations (such as the random-phase approximation (RPA)) must be used to include such time dependence. In the present approach, the nucleon--nucleon interaction is instead mediated by dynamical mesons, and time dependence arises naturally in response to the local hydrodynamic nuclear motion. Thus, the excita-

tions described here are *not* the result of collision-based equilibrium ("first sound"); they are instead composed of long-range coherent oscillations of the local Fermi surface ("zero sound") brought about by the changing meson fields.

As in Refs. [5] and [6], Bernoulli's equation relates ψ_p and ψ_n to appropriate chemical potentials μ_p and μ_n. Our chemical potentials differ from those of Walecka and Horowitz only by the addition of a Coulomb term:

$$\mu_p = g_v V_0 + \tfrac{1}{2} g_\varrho b_0 + eA_0 + (k_{F_p}^2 + M^{*2})^{1/2},$$
$$\mu_n = g_v V_0 - \tfrac{1}{2} g_\varrho b_0 + (k_{F_n}^2 + M^{*2})^{1/2}. \tag{1}$$

Here $M^* = M - g_s\phi_0$ defines the nucleon effective mass in terms of the nucleon mass M. The scalar, vector, and rho meson coupling constants are denoted by g_s, g_v, and g_ϱ; and ϕ_0, V_0, and b_0 are the corresponding meson fields. The Coulomb potential is A_0, and $\alpha = e^2/4\pi \approx 1/137$. The proton (neutron) Fermi wavenumber is $k_{F_p}(k_{F_n})$ and is specified in this model by $n_{p,n} = k_{F_{p,n}}^3/3\pi^2$ with $n_p(n_n)$ the proton (neutron) density. We use the units $\hbar = c = 1$ throughout.

The values of the input constants are given in Table I and are those used in the relativistic Hartree calculations of the nuclear ground states [4]. The three couplings g_s, g_v, g_ϱ, and the scalar meson mass m_s are determined by the saturation properties of infinite

TABLE I

Model parameters

Field	Meson	$J^\pi T$	Mass (MeV)	g^2	$C^2 \equiv g^2(M^2/m^2)$
ϕ	σ	0^+0	520	109.626	357.47
V_μ	ω	1^-0	783	190.431	273.87
b_μ	ϱ	1^-1	770	65.226	97.00

The parameters are determined from bulk nuclear ground-state properties as discussed in Ref. [4]. The nucleon mass is taken to be $M = 939$ MeV.

nuclear matter and the rms charge radius in ^{40}Ca; the resulting Hartree calculations provide a good description of the static properties of doubly magic nuclei. The parameters are not changed in this work and no new parameters are introduced to describe the collective oscillations.

The hydrodynamic equations used here are identical to those in Refs. [5] and [6], except that the Coulomb field is included. The nuclear motion is described by Bernoulli's equation:

$$-\frac{\partial \psi_p}{\partial t} + \tfrac{1}{2}(\nabla\psi_p)^2 + \frac{\mu_p}{M} = 0, \tag{2a}$$

$$-\frac{\partial \psi_n}{\partial t} + \tfrac{1}{2}(\nabla\psi_n)^2 + \frac{\mu_n}{M} = 0 \tag{2b}$$

and two continuity conditions:

$$\frac{\partial n_p}{\partial t} - \nabla \cdot (n_p \nabla \psi_p) = 0, \tag{3a}$$

$$\frac{\partial n_n}{\partial t} - \nabla \cdot (n_n \nabla \psi_n) = 0. \tag{3b}$$

The meson fields are specified by the local baryon sources:

$$(\partial_\mu \partial^\mu + m_v^2) V_0 = g_v (n_p + n_n), \tag{4a}$$

$$(\partial_\mu \partial^\mu + m_\varrho^2) b_0 = \tfrac{1}{2} g_\varrho (n_p - n_n), \tag{4b}$$

$$(\partial_\mu \partial^\mu + m_s^2) \phi_0 = g_s \frac{2}{(2\pi)^3} \left[\int_0^{k_{F_p}} + \int_0^{k_{F_n}} \right] \frac{M^* d^3 k}{(k^2 + M^{*2})^{1/2}} . \tag{4c}$$

In the Coulomb gauge, the potential A_0 is determined by Poisson's equation

$$-\nabla^2 A_0 = e n_p. \tag{5}$$

The static solutions to these equations reproduce the Thomas-Fermi results of Ref. [11], although in the present calculations, the ground-state densities are taken from the Hartree results. This is discussed in detail below.

To describe the collective oscillations, the boson fields and baryon densities are written as the sum of a static (ground-state) contribution plus a small, time-dependent increment, and we linearize Eqs. (1)–(5) about the equilibrium static solution. We then look for normal-mode excitations with harmonic time dependence, so that the increments take the form of the real parts of $\{i\delta\psi_p, i\delta\psi_n, \delta n_p, \delta n_n, \delta\phi_0, \delta V_0, \delta b_0, \delta A_0\} e^{-i\omega t}$. All quantities in braces are functions of the coordinate x.

The equations are simplified by assuming that the collective modes have much lower energy than the meson masses: $\omega^2 \ll m_s^2, m_v^2, m_\varrho^2$, which is clearly a good approximation for giant resonances ($\omega \lesssim 40$ MeV $\ll m_s \approx 500$ MeV). We also assume that the baryon density does not vary significantly over the Compton wavelength of the omega and rho mesons. This approximation is not essential, but it simplifies the calculations considerably. When this approximation was relaxed in several test cases, the quantitative results were changed by less than 5%, and the systematic A dependences discussed in Sect. 3 were virtually unchanged.

The preceding approximation reduces Eqs. (4a) and (4b) to

$$\delta V_0 = \frac{g_v}{m_v^2} (\delta n_p + \delta n_n), \quad \delta b_0 = \tfrac{1}{2} \frac{g_\varrho}{m_\varrho^2} (\delta n_p - \delta n_n). \tag{6}$$

Linearization of the other equations and substitution of (6) yields coupled eigenvalue equations in six unknowns:

Bernoulli's equations:

$$M\omega\delta\psi_p = \frac{g_v^2}{m_v^2}(\delta n_p+\delta n_n)+\tfrac{1}{4}\frac{g_\varrho^2}{m_\varrho^2}(\delta n_p-\delta n_n)+\frac{M^*}{\varepsilon_{F_p}}\delta M^*+\frac{\pi^2}{\varepsilon_{F_p}k_{F_p}}\delta n_p+e\delta A_0,$$

$$M\omega\delta\psi_n = \frac{g_v^2}{m_v^2}(\delta n_p+\delta n_n)-\frac{1}{4}\frac{g_\varrho^2}{m_\varrho^2}(\delta n_p-\delta n_n)+\frac{M^*}{\varepsilon_{F_n}}\delta M^*+\frac{\pi^2}{\varepsilon_{F_n}k_{F_n}}\delta n_p, \tag{7}$$

two continuity equations:

$$\nabla\cdot(n_p\nabla\delta\psi_p) = -\omega\delta n_p,$$

$$\nabla\cdot(n_n\nabla\delta\psi_n) = -\omega\delta n_n, \tag{8}$$

a scalar field equation:

$$\left\{\nabla^2-m_s^2-g_s^2\frac{2}{(2\pi)^3}\left[\int_0^{k_{F_p}}+\int_0^{k_{F_n}}\right]\frac{k^2d^3k}{(k^2+M^{*2})^{3/2}}\right\}\delta M^* = g_s^2M^*\left(\frac{\delta n_p}{\varepsilon_{F_p}}+\frac{\delta n_n}{\varepsilon_{F_n}}\right), \tag{9}$$

and a linearized Poisson's equation:

$$\nabla^2\delta A_0 = -e\delta n_p. \tag{10}$$

Here $\varepsilon_{F_{p,n}} = (k_{F_{p,n}}^2+M^{*2})^{1/2}$, and k_{F_p}, k_{F_n}, and M^* are determined from the equilibrium ground-state solution.

In deriving these results, contributions to the energy of order $(v/c)^2$ have been neglected in transforming from the rest frame of the nuclear fluid to the laboratory frame and by omitting the three-vector parts of the meson fields (as well as the electromagnetic vector potential $\boldsymbol{A}$). This is reasonable in view of the relatively low frequencies of the desired solutions. Equations (7)–(10) reduce to the results of Horowitz and Walecka [6] in the limit of $\alpha = 0$, $N = Z$, and equal ground-state densities for the neutrons and protons. The simplicity of this limit previously allowed exact numerical solution of these equations for the isovector case, in which the neutrons and protons oscillate against each other. The added complexity of the general case (corresponding to real nuclei) makes an exact numerical integration of the present equations more difficult. We therefore utilize the variational method described below.

3. Variational calculation

To estimate the eigenvalue of the lowest-energy mode with given angular momentum l, we use a variational approach [5]. This is preferable to a direct numerical integration of Eqs. (7)–(10) for several reasons. First, the coupled differential equations are difficult to solve numerically when $N \neq Z$ and $\alpha \neq 0$, as there is no exact separation into isoscalar and isovector modes. Second, since the hydrodynamic description of nuclear motion breaks down in the low-density region outside the nuclear surface, there are difficulties in defining the proper boundary conditions when realistic (exponentially decaying) ground-state densities are used. Finally, little is sacrificed in the variational approach if we are

interested in the lowest-lying modes. In the $N = Z$ limit, where exact solutions have been obtained for the isovector modes [6], variational estimates give the eigenvalues to within 5%. These solutions, together with other theoretical analyses (the phenomenological Tassie model [12], nonrelativistic RPA calculations, and fluid-dynamical models [8, 9]), allow us to construct simple yet realistic variational trial functions. By minimizing the computational effort, we can easily examine a wide variety of results to test the underlying physics and to determine if microscopic relativistic TDA or RPA calculations of excited states are warranted in the present model.

We therefore consider the minimization of the energy functional

$$E[\delta\psi_p, \delta\psi_n, \delta n_p, \delta n_n, \delta M^*, \delta A_0] = t[\delta\psi_p, \delta\psi_n] + v[\delta n_p, \delta n_n, \delta M^*, \delta A_0], \tag{11}$$

where

$$t = M \int d^3x \, \tfrac{1}{2} [n_p(\nabla\delta\psi_p)^2 + n_n(\nabla\delta\psi_n)^2], \tag{12a}$$

$$\begin{aligned} v = \int d^3x \Bigg\{ & \tfrac{1}{2} \frac{g_v^2}{m_v^2} (\delta n_p + \delta n_n)^2 + \tfrac{1}{8} \frac{g_\varrho^2}{m_\varrho^2} (\delta n_p - \delta n_n)^2 \\ & + M^* \left(\frac{\delta n_p}{\varepsilon_{F_p}} + \frac{\delta n_n}{\varepsilon_{F_n}} \right) \delta M^* + \tfrac{1}{2} \pi^2 \left(\frac{\delta n_p^2}{k_{F_p} \varepsilon_{F_p}} + \frac{\delta n_n^2}{k_{F_n} \varepsilon_{F_n}} \right) \\ & + \frac{1}{2g_s^2} \Bigg\{ (\nabla \delta M^*)^2 + \left(m_s^2 + g_s^2 \frac{2}{(2\pi)^3} \left[\int_0^{k_{F_p}} + \int_0^{k_{F_n}} \right] \frac{k^2 d^3k}{(k^2 + M^{*2})^{3/2}} \right) (\delta M^*)^2 \Bigg\} \\ & + e \delta A_0 \delta n_p - \tfrac{1}{2} (\nabla \delta A_0)^2 \Bigg\}, \end{aligned} \tag{12b}$$

subject to the constraint

$$M \int d^3x \delta\psi_p \delta n_p + M \int d^3x \delta\psi_n \delta n_n = 1. \tag{13}$$

This functional reduces to the one used by Horowitz and Walecka [6] when $\alpha = 0$. When the constraint is incorporated with a Lagrange multiplier ω, the Euler-Lagrange equations resulting from (12) are precisely Eqs. (7)–(10). (One must also assume natural boundary conditions $n\nabla\psi \to 0$ as $|x| \to \infty$ so that surface terms vanish.) By substituting the fields that satisfy these equations into (12) and carrying out several partial integrations, we may identify E with the eigenvalue ω. Thus variational estimates of the lowest eigenvalues may be obtained by minimizing E subject to the constraint.

Since E depends on six independent functions, a complete minimization is still quite difficult. To simplify the calculation, we use the following procedures, which are similar to those in Ref. [5]:

1) Notice that the scale transformation $\delta\psi \to d\delta\psi$, $\delta n \to d^{-1}\delta n$, $\delta A_0 \to d^{-1}\delta A_0$, and $\delta M^* \to d^{-1}\delta M^*$ leaves the constraint condition unchanged. Thus E can be minimized

immediately with respect to d^2. The result is

$$E_{\min} = 2(tv)^{1/2}, \tag{14}$$

which implies that the best estimate for E is found by minimizing the geometric mean of t and v. This is equivalent to minimizing E with respect to the relative normalizations of the densities δn and velocity potentials $\delta\psi$.

2) Following Walecka [5], we introduce a variational ansatz for δM^*:

$$\delta M^* = -a(\delta n_p + \delta n_n). \tag{15}$$

This assumes that on the average, the change in the scalar field is proportional to the change in the baryon density. This is true in nuclear matter at long wavelengths, and holds approximately in finite nuclei if the effect of the gradient in Eq. (9) is not large. Using (15), we may eliminate δM^* from the functional (11) and minimize directly with respect to the parameter a.

3) For the velocity potentials $\delta\psi_p$ and $\delta\psi_n$ describing a mode of angular momentum l, we choose a spatial dependence proportional to $x^p Y_{l0}(\Omega)$, where p is an (integer) variational parameter. This is the same form used by Horowitz and Walecka and yields a good approximation to the exact solutions for the velocity potentials found in Ref. [6]. Note that if the nucleus were an incompressible liquid drop, the exact solutions for modes of angular momentum l would behave as x^l, so we expect to find the variational value $p_{\min} \approx l$.

4) The relative sign of $\delta\psi_p$ and $\delta\psi_n$ is chosen according to the isospin character of the mode. Isoscalar modes have neutrons and protons moving in phase, so we choose $\delta\psi_p$ and $\delta\psi_n$ to have the same sign. Neutrons and protons move 180° out of phase for isovector modes, and we thus take $\delta\psi_p$ and $\delta\psi_n$ to have opposite signs. As discussed by Sagawa and Holzwarth [13], giant resonances correspond to constrained motion of the system, imposed by the external probe, rather than eigenmodes of excitation. The preceding sign choice (as well as $|\delta\psi_p| = |\delta\psi_n|$) follows from the connection between the transition operator and the velocity potential [10].

5) The density fluctuations δn_p and δn_n are given the same dependence on the radius and an angular dependence of $Y_{l0}(\Omega)$. For a given δn_p, Poisson's equation (10) is solved exactly for δA_0. After a partial integration, the Coulomb contribution to the energy functional reduces to

$$E_{\text{Coul}} = \int d^3x \, \tfrac{1}{2} e\delta A_0(x)\delta n_p(x) = \tfrac{1}{2}\frac{e^2}{4\pi}\int d^3x d^3x' \, \frac{\delta n_p(x)\delta n_p(x')}{|x-x'|}. \tag{16}$$

We further simplify the variation by taking $\delta n_n = b\delta n_p$ and determine b variationally from (12). This is a good approximation for all but the heaviest nuclei, where it may be necessary to also scale the radial dependence, as discussed below. In the $N = Z$ and $\alpha = 0$ limit, direct minimization of (11) leads to $b_{\min} = \pm 1$, which is independent of the radial form of δn_p. This represents, of course, an exact factorization of the isoscalar and isovector modes. In the general case, the variationally determined value of b is close to ± 1.

The basic ansatz for the density fluctuations is taken to be [5, 6]

$$\delta n_p = C\left(\frac{x}{x_0}\right)^q\left(1-\frac{x}{x_0}\right)Y_{l0}(\Omega), \quad \delta n_n = b\delta n_p, \tag{17}$$

where q is an integer variational parameter and x_0 is determined from the ground-state density, as described shortly. This ansatz gives good agreement with the exact transition densities found in Ref. [6]. The velocity potentials $\delta\psi_p$ and $\delta\psi_n$ are written as $\delta\psi = C(x/x_0)^p Y_{l0}(\Omega)$, with a relative sign specified by the isospin character of the mode. The increments in the Coulomb potential and effective mass are eliminated from E using Eqs. (15) and (16), the normalization constant C is eliminated using (13), and the resulting functional is minimized directly with respect to a. The energy functional then depends explicitly only on the ground-state nuclear densities, the variational parameters p and q describing the proton fluctuations, and the neutron/proton scale parameter b. These are determined numerically by minimizing the geometric mean of t and v (see Eq. (14)). Note that the conservation of protons implies $\int d^3x\delta n_p = 0$, which is automatically satisfied for $l > 0$. For monopole ($l = 0$) modes, we replace $(x/x_0)^q$ with $(x/x_0)^q - \xi$ and choose ξ to satisfy proton conservation.

One of the important features of the present investigation is the use of ground-state densities determined from relativistic Hartree calculations. This allows for a more accurate description of the nuclear interior and surface than in the Thomas-Fermi approach. Nevertheless, the Hartree densities have exponentially decaying tails at large radii, and the linearized hydrodynamic equations break down in this region. It is thus necessary to impose a cutoff radius x_0 on the variational trial functions and consequently in the integrals determining the energy functional. Since the dynamics of the collective modes is determined primarily by the nuclear surface, variational results should be insensitive to the cutoff, as long as it is chosen sufficiently far into the tail region. The quantitative effects of the cutoff are easily investigated by performing calculations for a range of reasonable values of x_0 (see the discussion in Sect. 4).

In physical terms, imposing a cutoff radius implies that only the particles in the nuclear core are accurately described by the hydrodynamic approximation. Thus, oscillations of the core are studied in the present approach. The least-tightly-bound nucleons contribute significantly to the nuclear tail, and their effects may be incorporated using a core-plus-valence model, as in Ref. [14]. (We have verified that the total number of nucleons outside of the cutoff x_0 is $\lesssim 1$ in calcium and $\lesssim 3$ in lead.) Alternatively, one can define a completely consistent dynamics using either a time-dependent Hartree approximation or an extended (nonlinear) version of the hydrodynamic equations. These approaches are beyond the scope of this initial investigation, but offer fruitful areas for future study.

To choose the cutoff x_0, the relations for the chemical potentials (1) are inverted using the static Hartree mean fields to determine "local" Fermi wavenumbers $k_{F_p}(x)$ and $k_{F_n}(x)$. This defines local proton and neutron densities that are similar to those in the Thomas-Fermi case. The chemical potentials μ_p and μ_n are chosen so that the volume integrals of these local densities reproduce the proper number of protons and neutrons.

The local densities are found to be nearly identical to exact Thomas-Fermi results in the nuclear surface, in cases where the latter have been calculated [11]. Moreover, the approximate local densities vanish at radii close to those obtained in the Thomas-Fermi calculations (see Fig. 1), and these radii are used to define reasonable ranges for x_0. The values of x_0 determined in this fashion are used to specify the variational trial functions and also to truncate the integrals over Hartree densities needed in the evaluation of (12).

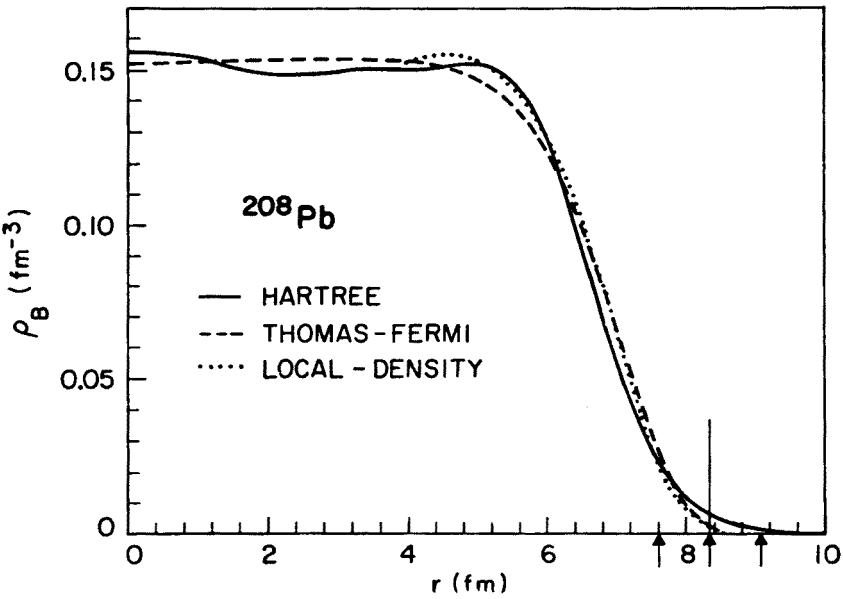

Fig. 1. Ground-state baryon density of ^{208}Pb. Relativistic Hartree results [4] are indicated by the solid curve, and the Thomas-Fermi calculations [11] are denoted by the dashed curve. The dotted curve is the local density found by inverting the chemical potentials as described in Sect. 3. The three arrows show several choices of cutoff radii. The central arrow gives the average of neutron and proton cutoffs for ^{208}Pb [$x_0 = \frac{1}{2}(x_{0p}+x_{0n}) = 8.35$ fm], which was used to calculate the results in Table II and Fig. 4. The other two arrows show the minimum and maximum cutoff radii used to study the sensitivity of variational results

The sensitivity of the variational results was tested by varying the cutoff radii over a reasonable range and also by allowing different cutoffs x_{0n} and x_{0p} for neutrons and protons in Eq. (17). (This introduces a scaling of the radial dependence in the proton and neutron trial functions.) Detailed results will be discussed in the next section. As a further check, an alternative density trial function of the form

$$\delta n_p = Cx^q \frac{dn_p}{dx} Y_{l0}(\Omega), \quad \delta n_n = bCx^q \frac{dn_n}{dx} Y_{l0}(\Omega) \tag{18}$$

was used. This is a generalization of the Tassie model result [12], where $\delta n \sim x^{l-1}(dn/dx) \times Y_{l0}(\Omega)$. We thus expect to find $q_{\min} \approx l-1$ for isoscalar modes. Since the relative magnitude of the neutron and proton fluctuations is built into the ansatz, we also expect $|b_{\min}|$

to be close to unity. For monopole modes, we used

$$\delta n_p = Cx^{q-1}\left[x\frac{dn_p}{dx} + (q+2)n_p\right]Y_{l0}(\Omega),$$

$$\delta n_n = bCx^{q-1}\left[x\frac{dn_n}{dx} + (q+2)n_n\right]Y_{l0}(\Omega), \tag{19}$$

to automatically satisfy $\int d^3x\delta n = 0$. Recent fluid dynamical calculations of collective modes show good agreement between Tassie model predictions and more elaborate calculations of transition densities [15]. When this alternative ansatz was used with the model nucleus of Refs. [5] and [6], the variational energies were modified by less than 1%. For the present calculations with Hartree densities, a cutoff must again be imposed, but variational estimates were found to be relatively insensitive to the precise value of x_0.

4. Results and discussion

Energies of the lowest-lying isoscalar and isovector modes for $0 \leqslant l \leqslant 4$ were found for ^{40}Ca, ^{48}Ca, ^{90}Zr, and ^{208}Pb using the ground-state Hartree densities of Ref. [4]. A summary of results is given in Table II, and representative energy spectra are compared with experiment in Figs. 2–4. The systematic A dependence of the eigenvalues is illustrated in Figs. 5–7, where we plot excitation energy times $A^{1/3}$ as a function of the baryon number. These results were calculated with the trial function of Eq. (17) and equal cutoff radii for neutrons and protons. The cutoff radius was determined by inverting Eqs. (1) as described in Section 3 and averaging the values obtained for neutrons and protons: $x_0 = \frac{1}{2}(x_{0p}+x_{0n})$. Theoretical error bars indicate changes obtained when the cutoffs are varied about the values determined from this procedure and when different cutoffs are used for protons and neutrons. The sensitivity of the energies to these variations is discussed below.

TABLE II

Variational collective mode energies (in MeV)

	^{40}Ca	^{48}Ca	^{90}Zr	^{208}Pb
Isoscalar $l = 0$	47.4	44.6	38.7	28.1
2	21.5	20.1	16.9	11.8
3	30.9	28.1	23.8	16.3
4	39.9	36.4	30.5	20.8
Isovector $l = 0$	34.9	33.9	32.2	27.2
1	17.2	16.8	15.1	12.3
2	23.4	22.9	21.1	17.6
3	27.8	26.9	25.4	21.5
4	31.6	30.5	28.9	24.7

Variational estimates of eigenvalues for the lowest mode with a given angular momentum l. The trial function in Eq. (17) was used with equal proton and neutron cutoffs.

Giant resonances of several multipolarities are observed in most medium and heavy nuclei. The experimental energies [16] follow systematic trends that are indicated in Figs. 5–7. The A dependence of the variational results is similar to experimental values, and the eigenvalues agree with experiment to within approximately 20% for all but the isoscalar monopole. Reasonable variations in the cutoff radii may change the absolute energies by $\pm 10\%$ but do not appreciably modify the systematic trends.

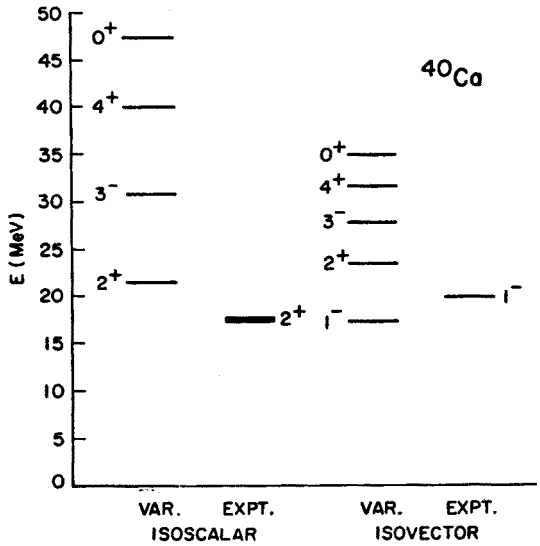

Fig. 2. Energy spectrum of collective modes for ^{40}Ca. Variational estimates are from Table II and experimental levels are from Ref. [16]. Experimental uncertainties are indicated by shading

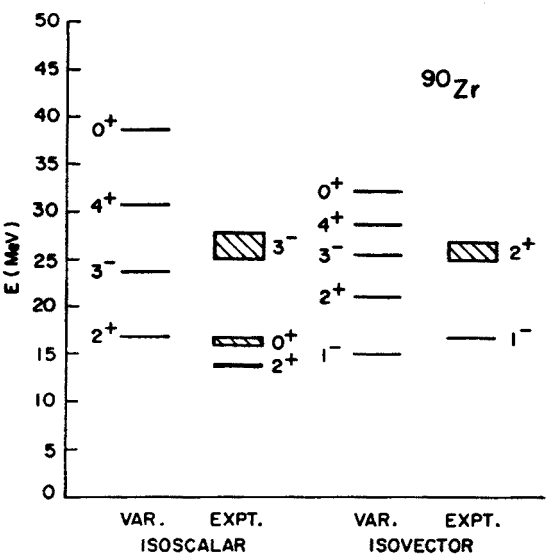

Fig. 3. Same as Fig. 2 for ^{90}Zr

The qualitative agreement of the present calculations with experimental systematics is an important result. As Bertsch [10] and others [15, 17] have noted, nonrelativistic hydrodynamic models predict incorrect systematics — for example, isoscalar quadrupole excitation energies that scale as $A^{-1/2}$. Evidently, the collective modes found here are not simply the surface oscillations of an incompressible liquid drop [18]. Despite the simplicity of our approach, a significant part of the underlying dynamics is retained through the interaction of the nucleons with the oscillating meson fields.

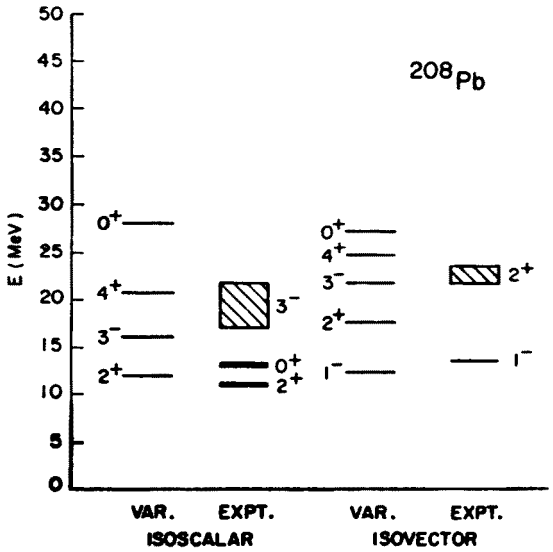

Fig. 4. Same as Fig. 2 for ^{208}Pb

The systematics of the isovector dipole excitation are in good agreement with the data, with variational eigenvalue lying 10–20% below experimental results. The isoscalar energies scale approximately as $A^{1/3}$, with the quadrupole results about 15% higher than experiment and the octupole energies slightly lower than the data. We again remark that the small number of input parameters are determined from static nuclear matter properties; no new parameters were introduced to improve the present dynamical calculations.

The isoscalar monopole excitation is a compressional mode, and its energy is related to the compressibility of nuclear matter [19]. As previously noted [4], the compressibility in the current model is too high by about a factor of two, and consequently, the calculated monopole energies are significantly greater than experimental values.

In general, we find that the calculated isovector levels are lower than experiment, while the isoscalar results lie higher. The calculated isospin splittings for the quadrupole mode are therefore substantially less than those observed in real nuclei. There are two distinct reasons for this discrepancy. First, the oscillation of the local effective mass $M^*(r)$ in isoscalar modes leads to a sensitive cancellation between the repulsive $(\delta n)^2$ and $(\delta M^*)^2$

terms and the attractive cross term $\delta n \delta M^*$ in the potential energy functional v (see Eq. (12b)). The variational ansatz for this oscillation (Eq. (15)) and the truncated Hartree ground-state densities reproduce this cancellation only approximately. This has been verified by evaluating the variational energy of the (spurious) isoscalar dipole mode, which occurs at 5 to 10 MeV (rather than at zero energy). Thus the isoscalar mode energies are overestimated by similar amounts.

In contrast, the isovector modes involve almost no change in the local effective mass, since the neutron and proton densities oscillate essentially out of phase [6]. The underestimation of the isovector energies may therefore be related to the symmetry energy. In the static solutions, the proper symmetry energy can be obtained by choosing the rho meson coupling appropriately [4]. It is known, however, that a significant contribution to the symmetry energy of nuclear matter arises from exchange contributions that are neglected

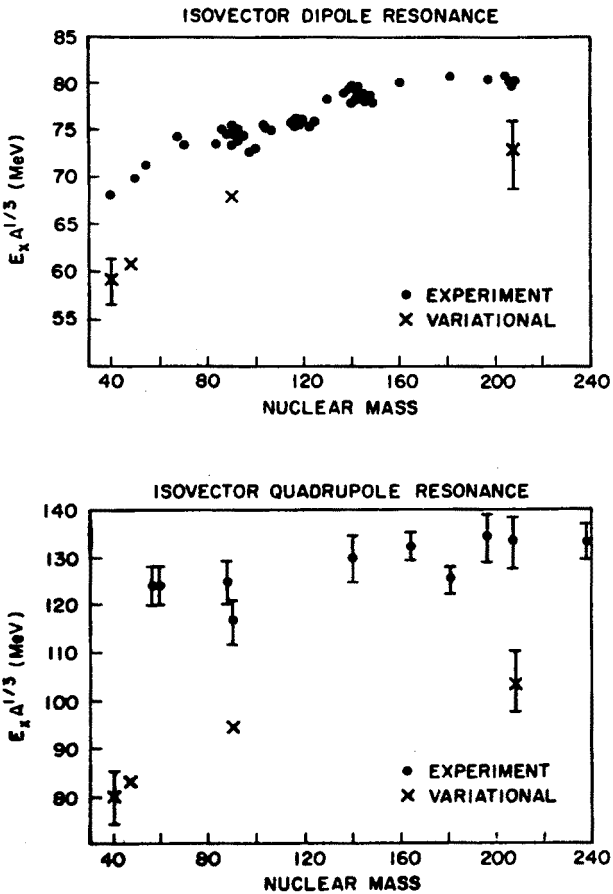

Fig. 5. Systematics of isovector dipole and quadrupole resonances. Experimental data are from Ref. [16]. Theoretical error bars indicate variations in excitation energy for different choices of cutoffs, as described in the text

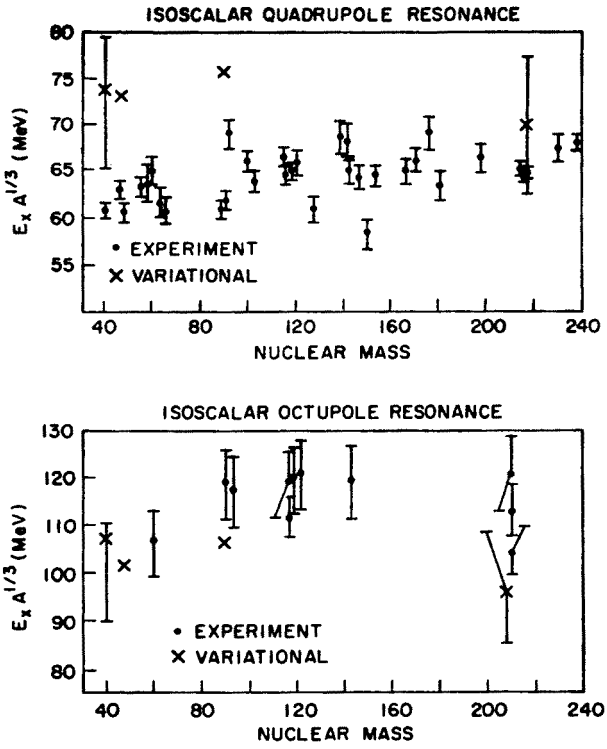

Fig. 6. Systematics of isoscalar quadrupole and octupole giant resonances. Experimental data are from Ref. [16]

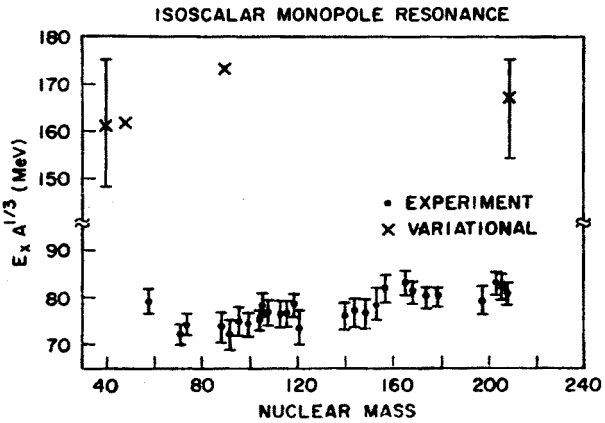

Fig. 7. Systematics of isoscalar monopole giant resonance. Experimental data are from Ref. [16]. Note the broken vertical scale

in the present formalism [20]. These additional contributions may be required to achieve a correct symmetry energy for the dynamical modes. Both of the preceding features in our simple approach are expected to improve in more sophisticated calculations.

If we compare the results for the model nucleus ($A = 67.19$) of Refs. [5] and [6] to the systematic trends by scaling with appropriate factors of $A^{1/3}$, we find similar results for the isovector modes. The isoscalar levels, however, are considerably higher (up to 50%) in the present calculations. This can be attributed primarily to the different meson masses and coupling constants. The net potential energy contributions of the scalar

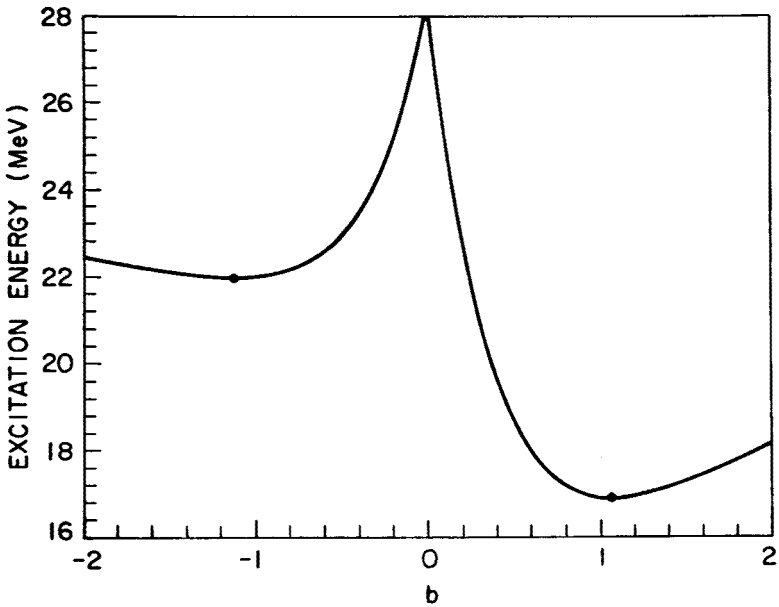

Fig. 8. Excitation energy for quadrupole modes in ^{90}Zr as a function of neutron/proton scale parameter b. The variational parameters $p = 2$ and $q = 4$ are held fixed. The dots mark the values of b at the local minima in the energy functional. (These p and q values are chosen for illustration and do not lead to the absolute minimum energies for these modes.)

and vector meson field fluctuations (see Eq. (12b)) are determined by these values. The constants in the present case accurately predict the static properties of real nuclei.

Turning now to the effect of the Coulomb potential, we find that the incremental Coulomb energy is small compared to the other contributions. Even in lead, it contributes only a few percent of the total potential energy v in Eq. (12). Although the effect of the Coulomb potential on individual isoscalar and isovector modes is difficult to determine quantitatively, setting α to zero leads to only small modifications in the results presented above.

As expected, the magnitude of the variational parameter b, which determines the relative normalization of neutron and proton fluctuations, is approximately equal to

unity for light nuclei ($N = Z$) and between unity and N/Z for the others[1]. In Fig. 8, an example of the excitation energy as a function of b (for fixed p and q) illustrates the distinct isoscalar ($b > 0$) and isovector ($b < 0$) minima.

Finally, we consider changes in the eigenvalues when the cutoff radii and variational trial functions are varied. For equal neutron and proton cutoffs, energies of the lower multipoles change by 10–15% for reasonable variations (approximately $\pm\frac{1}{2}$ fm in lead and $\pm\frac{1}{4}$ fm in calcium), with isoscalar energies more sensitive than isovector energies because of the sensitive cancellations involved in the former. The isovector dipole modes are the least sensitive to the cutoff radius. Similar results are obtained when different proton and neutron cutoffs are used. The higher multipoles are more sharply peaked at the nuclear surface and are consequently more sensitive to the cutoff values. We remark that although calculations based on Thomas-Fermi ground-state densities have a well-defined cutoff radius, there is similar sensitivity to the precise location of the nuclear edge. Calculations were also carried out with the alternative trial function of Eqs. (18) and (19). Energy eigenvalues agreed with those of the basic ansatz (17) to within 10%, and the minimized transition densities had similar shapes. The p and q values for the isoscalar modes agreed with those predicted in the Tassie model, namely, $p_{\min} \approx l$ and $q_{\min} \approx l-1$.

5. *Inelastic electron scattering*

Normalized transition densities are needed to describe inelastic electron-nucleus scattering [18, 21]. Since we work with linearized field equations, the normalizations are not determined by the preceding formalism. To specify the correct normalization for the collective modes, we follow a procedure analogous to that in Ref. [6].

First, a hamiltonian describing the collective dynamics is derived by eliminating meson and neutron degrees of freedom using the variational simplifications described in Sect. 3. The dynamics is then completely specified by δn_p and $\delta\psi_p$, and the system is quantized by interpreting these as operators with canonical commutation relations. Finally, we equate the hamiltonian H (which is a functional of δn_p and $\delta\psi_p$) to the normal-mode expression

$$H = \sum_n \omega_n \tfrac{1}{2}(a_n^\dagger a_n + a_n a_n^\dagger). \tag{20}$$

This procedure fixes the normalization of the transition density.

We begin with the lagrangian density $\mathscr{L}_2$ given in Eq. (31) of Ref. [6]. This describes (in lowest order) the dynamics of the collective modes in this model. The Euler-Lagrange equations resulting from $\mathscr{L}_2$ are the linear equations of motion presented in Sect. 2, and, for simplicity, Coulomb terms are neglected here (their contribution is not significant). The vector meson fields δV_0 and δb_0 are eliminated in favor of δn_p and δn_n using Eq. (6). δM^* is replaced using Eq. (15), where we consider the parameter a to be determined

[1] This is for equal proton and neutron cutoffs. Otherwise an overall scaling factor is included in b, as is clear from Eq. (17).

from the variational calculation. The neutron fluctuations are similarly replaced by proton fluctuations according to $\delta n_n = b\delta n_p$ and $\delta\psi_n = s\delta\psi_p$, where b is determined from the variational results and $s = \pm 1$ is specified by the isospin character of the mode. (All results in this section are for equal neutron and proton cutoff radii.)

The result is a lagrangian density $\overline{\mathscr{L}}_2$, which is quadratic in δn_p and $\delta\psi_p$:

$$\overline{\mathscr{L}}_2 = -\frac{(1+|b|)^2}{2M^2} W(x)\delta n_p^2 + M\left\{(1+|b|)\delta n_p \frac{\partial\delta\psi_p}{\partial t} - \tfrac{1}{2}[n_p + b^2 n_n](\nabla\delta\psi_p)^2\right\}, \quad (21)$$

where

$$W(x) = \left(C_v^2(1+b)^2 + \tfrac{1}{4}C_\varrho^2(1-b)^2 - aM^*M^2(1+b)\left(\frac{1}{\varepsilon_{F_p}} + \frac{b}{\varepsilon_{F_n}}\right)\right.$$
$$\left. + M^2\pi^2\left[\frac{1}{\varepsilon_{F_p}k_{F_p}} + \frac{b^2}{\varepsilon_{F_n}k_{F_n}}\right]\right)(1+|b|)^{-2} \quad (22)$$

and

$$C_i^2 = g_i^2(M^2/m_i^2).$$

This provides an approximate description of the collective motion, in that the meson and neutron fluctuations are related to the proton fluctuations in the same manner as in the variational calculations of Sect. 3. The proton fluctuations satisfy the Euler-Lagrange equations

$$M\omega\delta\psi_p = \frac{W(x)(1+|b|)}{M^2}\delta n_p, \quad (23)$$

$$\nabla\cdot[(n_p + b^2 n_n)\nabla\delta\psi_p] = -\omega(1+|b|)\delta n_p. \quad (24)$$

The corresponding hamiltonian density $\overline{\mathscr{H}}_2$ follows immediately from (21):

$$\overline{\mathscr{H}}_2 = \frac{(1+|b|)^2}{2M^2} W(x)\delta n_p^2 + \tfrac{1}{2}M[n_p + b^2 n_n](\nabla\delta\psi_p)^2, \quad (25)$$

and the hamiltonian is simply the volume integral of $\overline{\mathscr{H}}_2$,

$$H = \int d^3x\,\overline{\mathscr{H}} = \int d^3x\left(\frac{(1+|b|)^2}{2M^2} W(x)\delta n_p^2 + \tfrac{1}{2}M[n_p + b^2 n_n](\nabla\delta\psi_p)^2\right). \quad (26)$$

Proceeding as in Ref. [6], we expand the proton density fluctuation and velocity potential in normal-mode solutions of the Euler-Lagrange equations (23) and (24). In the Schrödinger representation, we find the time-independent field operators δn_p and $\delta\psi_p$:

$$\delta n_p = \sqrt{\tfrac{1}{2}}\sum_{nlm}[(\delta n_p)_{nl}Y_{lm}\hat{a}_{nlm} + \text{h.c.}],$$
$$\delta\psi_p = i\sqrt{\tfrac{1}{2}}\sum_{nlm}[(\delta\psi_p)_{nl}Y_{lm}\hat{a}_{nlm} - \text{h.c.}], \quad (27)$$

where $[\hat{a}_{nlm}, \hat{a}^{\dagger}_{nlm}] = 1$. (All other commutators are zero.) The hermitian conjugates (h.c.) are added to make the increments real. The Euler-Lagrange equations (23) and (24) may be combined to yield ($\bar{n} \equiv n_p + b^2 n_n$)

$$\bar{n}(\delta\psi_p)_l'' + \left(\frac{2\bar{n}}{x} + \bar{n}'\right)(\delta\psi_p)_l' - \frac{l(l+1)}{x^2}\bar{n}(\delta\psi_p)_l = \frac{-M^3\omega^2(\delta\psi_p)_l}{W(x)}, \tag{28}$$

which is of Sturm-Liouville form and implies

$$\int \frac{1}{W(x)}(\delta\psi_p)^*_{n'l}(\delta\psi_p)_{nl}x^2dx = \delta_{nn'}\frac{1}{M^4\omega_{nl}},$$

$$\int W(x)\,(\delta n_p)^*_{n'l}(\delta n_p)_{nl}x^2dx = \delta_{nn'}\omega_{nl}M^2(1+|b|)^{-2}. \tag{29}$$

It is easily verified that when substituted into (26), the normal-mode expansions and normalization conditions lead to (20).

In Fig. 9, normalized proton transition densities are shown for isovector modes in lead. Transition densities for the lighter nuclei are similar. Note that as the multipolarity l is increased, the peak in the density moves to larger radii, as expected. In Fig. 10, the proton transition density for the isoscalar quadrupole excitation in ^{208}Pb is compared with the corresponding result of a nonrelativistic RPA calculation [9].

To describe inelastic electron scattering, we use the plane-wave Born approximation (PWBA) [18, 21]. For quantitative comparison with experimental data, theoretical form

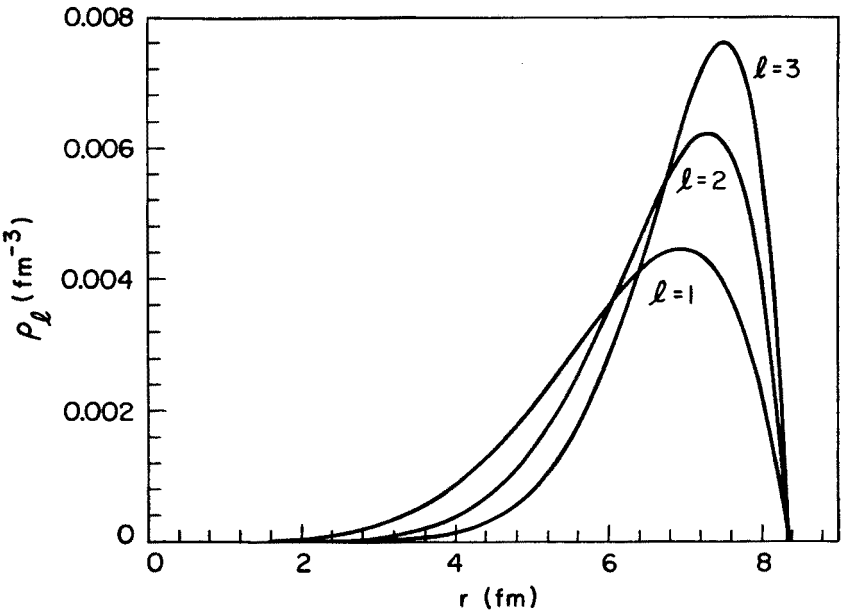

Fig. 9. Proton transition densities for isovector modes in ^{208}Pb. The variational trial functions are from Eq. (17) and are normalized as described in Sect. 5

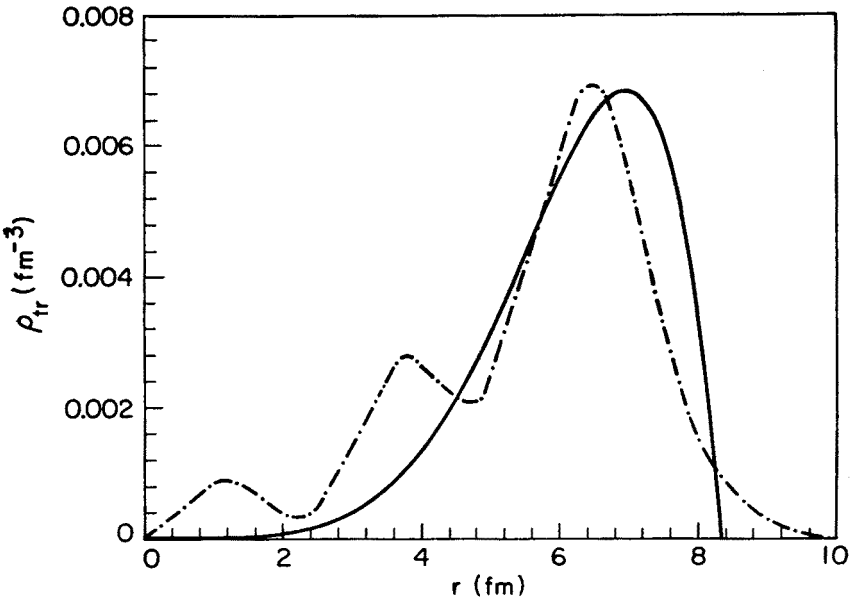

Fig. 10. Proton transition densities for the isoscalar quadrupole giant resonance in ^{208}Pb. The solid line is the normalized variational result. The dotdash line is a nonrelativistic RPA calculation of the surface oscillation contribution that dominates the 2^+ state

factors are usually calculated in the distorted-wave Born approximation (DWBA), particularly for heavy nuclei [22]. Since the present approach has uncertainties at the 10–20% level, the PWBA analysis is sufficient and more transparent. This simplification also allows us to use the formalism in Ref. [6], and we merely quote relevant results.

The Coulomb form factor for an excitation of an isolated state $|nL\rangle$ is given by

$$f_C^2(q) = \frac{2L+1}{2}\left[\int_0^{x_0} dx x^2(\delta n_p(x))_{nL} j_L(qx)\right]^2, \tag{30}$$

where, for simplicity, we consider only the transition charge density arising from point protons. It is straightforward to include the proton charge form factor, as discussed in Ref. [4]. For the transverse form factor, we include only the convective contributions of the protons, with the result

$$f_T^2(q) = L(L+1)(2L+1)\frac{1}{2q^2}\left[\int_0^{x_0} dx x(\delta\psi_p(x))_{nL}\left(\frac{dn_p}{dx}\right) j_L(qx)\right]^2. \tag{31}$$

Representative results are shown in Figs. 11 through 14.

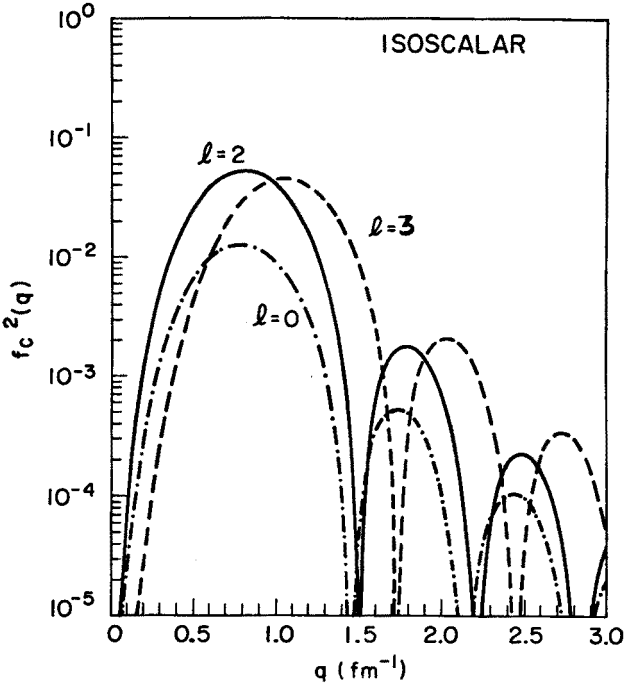

Fig. 11. Isoscalar Coulomb form factors $f_C^2(q)$ [see Eq. (30)] for ^{40}Ca for $L = 0$ (dotdash), $L = 2$ (solid), and $L = 3$ (dashed)

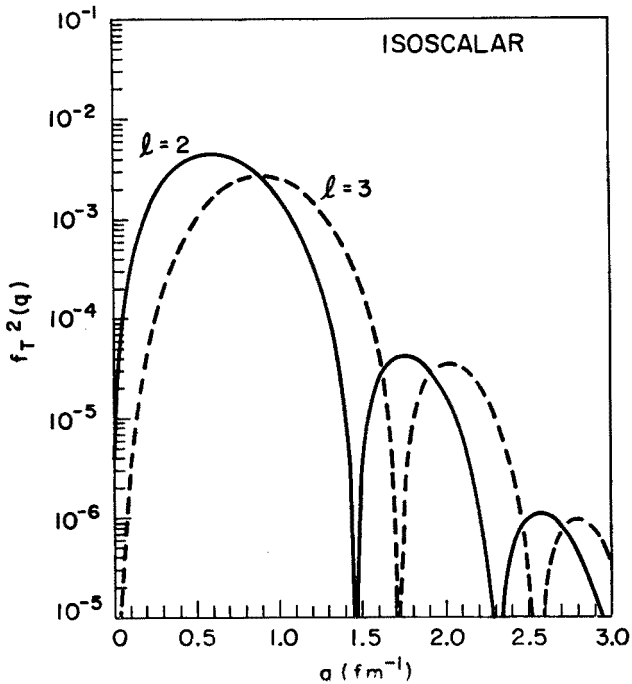

Fig. 12. Isoscalar transverse form factors $f_T^2(q)$ [see Eq. (31)] for ^{40}Ca for $L = 2$ (solid) and $L = 3$ (dashed)

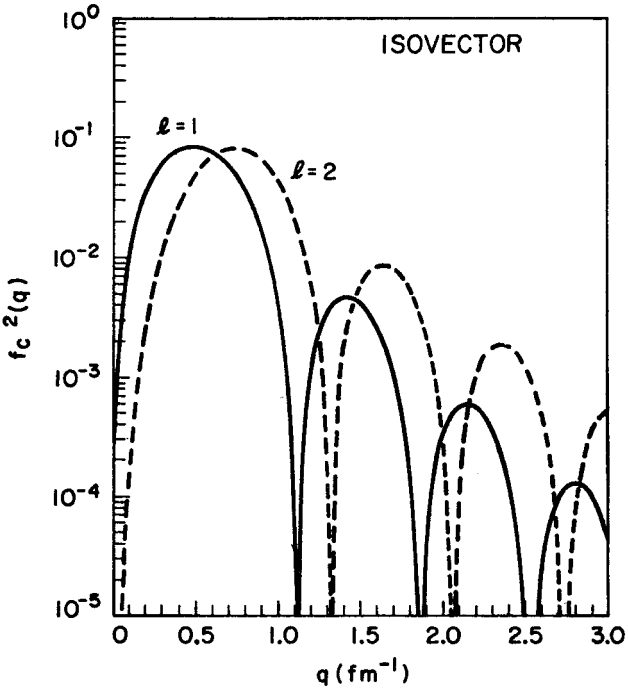

Fig. 13. Isovector Coulomb form factors $f_C^2(q)$ for ^{40}Ca for $L = 1$ (solid) and $L = 2$ (dashed)

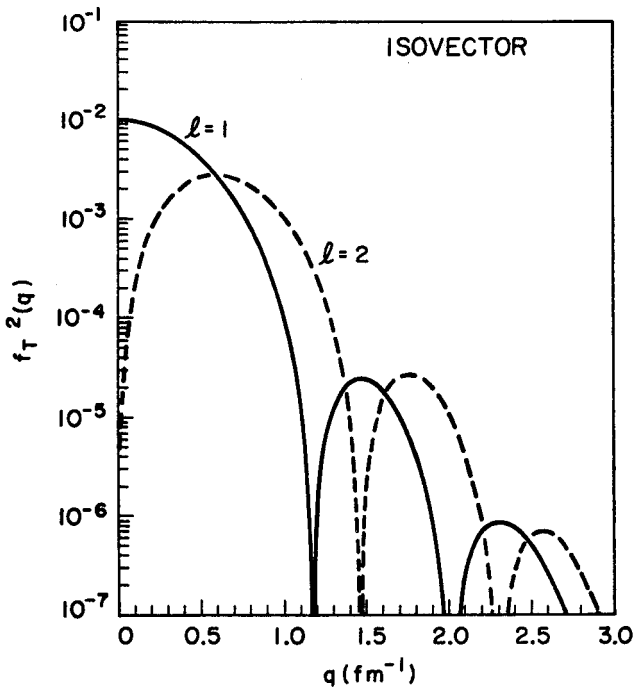

Fig. 14. Isovector transverse form factors $f_T^2(q)$ for ^{40}Ca for $L = 1$ (solid) and $L = 2$ (dashed)

The lowest state of each multipolarity exhausts a large fraction of the corresponding energy-weighted sum rule [9]. For example, the dipole states in ^{40}Ca, ^{48}Ca, ^{90}Zr, and ^{208}Pb exhaust 99%, 85%, 85%, and 65%, respectively, of the Thomas-Reiche-Kuhn sum rule. This reflects the highly collective nature of these modes.

6. *Summary*

We have described isovector and isoscalar collective modes in a relativistic mean-field theory by adding small time-dependent fluctuations to the ground-state meson fields and nucleon densities. Local hydrodynamic variables were introduced to describe the nucleon fluids, and the equations of motion were linearized about the static configurations. Variational estimates to the solutions of these equations were obtained using relativistic Hartree results to define the equilibrium densities. Energies and transition densities were found for the lowest-lying collective modes in the doubly magic nuclei ^{40}Ca, ^{48}Ca, ^{90}Zr, and ^{208}Pb.

One key feature of the present approach is its simplicity. *With parameters determined completely from the bulk properties of the static solutions,* reasonable results were predicted for the excited states. The calculation is self-consistent in this sense and leads to the important conclusion that *the large Lorentz scalar and vector components responsible for the ground-state properties are also compatible with collective nuclear excitations.* Because the mesons mediating the nucleon-nucleon interaction are inherently dynamical, time-dependent oscillations of the nucleus arise in a very simple and transparent manner. In addition, the use of a simple variational principle to describe the motion allows for systematics to be examined with a minimum of computational effort.

The main limitations of the present approach are discussed in detail by Horowitz and Walecka [6]. The use of local hydrodynamic variables, the assumption of irrotational flow, the linearization of the field equations, the limit of large masses for the vector mesons, and the variational method are all of limited accuracy. Nevertheless, this simple framework describes collective modes that display the qualitative features of giant resonances and follow the experimental systematics very reasonably. Thus a more sophisticated calculation has the promise of yielding accurate quantitative predictions.

There are two alternative directions in which to improve the present calculations. It may be feasible to extend the hydrodynamical description to include higher-order corrections and thus be more compatible with the exponential decay of the Hartree ground-state densities at large radii. Several nonrelativistic fluid-dynamical formalisms have recently been developed and have had some success in describing giant resonances [15, 17]. While this approach is computationally simpler than a true microscopic calculation, it has not been useful for describing detailed quantitative features of the excitations [8].

Alternatively, since the relativistic Hartree approximation successfully describes the ground state, a microscopic TDA or RPA calculation based on the resulting nucleon-nucleon interaction may be accurate. Nonrelativistic RPA calculations have been successful in predictions of centroid energies, transition probabilities, and reaction cross

sections, and one has the advantage of obtaining a more complete spectrum of the low-lying excitations [8, 9]. In many of these calculations, however, the residual nucleon-nucleon interaction is adjusted to reproduce some empirical properties of excited states. One benefit of the present approach is that an interaction determined entirely from ground-state properties could be used. Work is currently in progress on this topic.

The authors are pleased to acknowledge useful discussions with Professors G. F. Bertsch, C. J. Horowitz, and J. D. Walecka.

REFERENCES

[1] J. D. Walecka, *Ann. Phys.* (USA) **83**, 491 (1974).
[2] J. A. McNeil, J. Shepard, S. J. Wallace, *Phys. Rev. Lett.* **50**, 1439 (1983); B. C. Clark, S. Hama, R. L. Mercer, L. Ray, B. D. Serot, *Phys. Rev. Lett.* **50**, 1644 (1983).
[3] B. D. Serot, *Phys. Lett.* **86B**, 146 (1979); **87B**, 403 (E) (1979); B. D. Serot, Ph. D. Thesis, Stanford University 1979, unpublished.
[4] C. J. Horowitz, B. D. Serot, *Nucl. Phys.* **A368**, 503 (1981).
[5] J. D. Walecka, *Phys. Lett.* **94B**, 293 (1980).
[6] C. J. Horowitz, J. D. Walecka, *Nucl. Phys.* **A364**, 429 (1981).
[7] F. E. Serr, *Phys. Lett.* **97B**, 180 (1980); F. E. Serr, G. F. Bertsch, J. Borysowicz, *Phys. Lett.* **92B**, 241 (1980); F. E. Serr, T. S. Dumitrescu, T. Suzuki, C. H. Dasso, *Nucl. Phys.* **A404**, 359 (1983).
[8] K. Goeke, J. Speth, *Ann. Rev. Nucl. Part. Sci.* **32**, 65 (1982).
[9] J. Speth, A. van der Woude, *Rep. Prog. Phys.* **44**, 719 (1981).
[10] G. F. Bertsch, *Phys. Rev.* **C10**, 933 (1974); G. F. Bertsch, *Nucl. Phys.* **A249**, 253 (1975).
[11] B. D. Serot, J. D. Walecka, *Phys. Lett.* **87B**, 172 (1979).
[12] L. J. Tassie, *Aust. J. Phys.* **9**, 407 (1956).
[13] H. Sagawa, G. Holzwarth, *Prog. Theor. Phys.* **59**, 1213 (1978).
[14] J. D. Walecka, *Phys. Lett.* **58A**, 83 (1976); F. E. Serr, *Phys. Lett.* **62A**, 325 (1977).
[15] G. Eckart, G. Holzwarth, J. P. da Providencia, *Nucl. Phys.* **A364**, 1 (1981); G. Holzwarth, G. Eckart, *Nucl. Phys.* **A396**, 171c (1983).
[16] F. Bertrand, Proc. of Int. Conf. on Nuclear Physics, Berkeley, Calif. 1980, p. 129c.
[17] G. Holzwarth, G. Eckart, *Z. Phys.* **A284**, 197 (1978).
[18] T. DeForest, Jr., J. D. Walecka, *Adv. Phys.* **15**, 1 (1966).
[19] J. P. Blaizot, *Phys. Rep.* **64C**, 171 (1980).
[20] C. J. Horowitz, B. D. Serot, *Nucl. Phys.* **A399**, 529 (1983).
[21] T. W. Donnelly, J. D. Walecka, *Ann. Rev. Nucl. Sci.* **25**, 329 (1975).
[22] J. Heisenberg, *Adv. Nucl. Phys.* **12**, 61 (1981).